Synthesis and characterization of NiO nanoparticles prepared via plasma jet method

B. K. Al-Rawi [a,*], M. Kh. Ibrahem [b]
[a] *Department of Physics, College of Education for Pure Science, University of Anbar, Anbar, Iraq*
[b] *Ministry of Education, Anbar Education Directorate, Anbar, Iraq*

Nanomaterials have attracted significant attention due to their broad range of applications, particularly in electronics, catalysis, energy storage, and environmental remediation. The synthesis method plays a crucial role in determining the structural, morphological, and optical properties of these materials. In this work, nickel oxide (NiO) nanoparticles were synthesized using a plasma jet method, which offers advantages in terms of simplicity, environmental friendliness, and scalability. The purity of the synthesized NiO nanoparticles was confirmed through X-ray diffraction (XRD) and energy-dispersive X-ray (EDX) analysis. XRD analysis revealed characteristic peaks at 2θ = 37.2°, 43.3°, 62.9°, and 75.4°, which correspond to the (111), (200), (220), and (311) planes, respectively—a fingerprint of the cubic face-centered crystal structure of NiO. The average crystallite size calculated from the XRD data using the Scherrer equation was approximately 14.02 nm. Atomic force microscopy (AFM) provided surface topology data, from which the average particle size was estimated to be 72.65 nm, indicating some degree of agglomeration or grain stacking. Additionally, field emission scanning electron microscopy (FESEM) images confirmed the spherical morphology and good dispersion of the nanoparticles, with particle sizes ranging from 19.33 to 38.21 nm. Optical properties were investigated via UV-Vis spectroscopy, and the optical band gap energy (Eg) was calculated using a Tauc plot. The estimated band gap for the NiO nanoparticles was 4.05 eV, highlighting their potential for use in optoelectronic and photocatalytic applications.

(Received June 13, 2025; Accepted August 21, 2025)

Keywords: NiO, Plasma jet, Optical properties, Structural features

1. Introduction

Nanoparticles are a hot topic in science, and for good reason; as the mechanical, optical, and thermal properties of substances change with size, nanoparticles provide a unique opportunity to gain understanding into phenomena occurring at the nanoscale. These particles are usually defined as having diameters less than 100 nanometres. Metal nanoparticles are widely used for the advancement of many fields, including but not limited to biosensing, biomedical science, cosmetics, food technology, electronics, and medicine. The astonishingly combined electro-optical-catalytic-thermal properties at nanoscale levels offer significant interest for researchers to hybridize different components to form new mixed materials [1–3]. Many different Characteristics materials have the same effects on reducing the particle size from bulk to the nanoscale so these singular and advanced characteristics cause increase in the surface-to-volume ratio and change the behaviour clearly [4–6]. Materials based on nano-structured metal oxide have a variety of versatile properties, such as optical, magnetic, electrical, and catalytic properties. These extraordinary properties have gained a lot of attention which leads to many innovative applications in diverse areas [7].

Nickel oxide (NiO) is considered as one of the most chemically stable one. This cheap yet excellent ion storing capacity made it one of the most researched compounds [8]. The p-type conductivity of Nickel oxide nanoparticles is due to their high energy band gap (3.6 eV - 4.0 eV) [9, 10]. NiO NPs nanoparticles are extensively utilized in photocatalysis, batteries, electrochromic devices and chemical sensors. [11–13] and gas sensors [14]. There are different ways for preparing

* Corresponding author: sc.bilal_alrawi@uoanbar.edu.iq
https://doi.org/10.15251/DJNB.2025.203.987

nanoparticles namely PLD, sol–gel, chemical coprecipitation, thermal decomposition, and hydrothermal methods [15–17]. Recently, plasma technology has gained significant attention as a green nanomaterial preparation method and represents a new class of nanomaterial synthesis owing to its unique benefits compared with conventional solid, liquid and gas-phase syntheses [18]. A plasma jet is a low-temperature atmospheric pressure plasma and its afterglow (or plume, projectile, or stream) emerges from the plasma generator's nozzle tip [19]. Due to the high optical transparency of NiO thin films, they have significant value in optoelectronics. And changing their architecture, these films can also be modified for medical applications to enhance their antimicrobial or to serve as a platform for accurate drug delivery and biointerfacing. All of these properties make them suitable for use in antimicrobial coatings On medical devices, wound dressings, as well as regulation systems for controlled and targeted drug delivery [20]. In this analysis, nickel oxide nanoparticles will be produced by the plasma jet method and their optical and structural properties will be analyzed.

2. Experimental work

Figure 1 Schematic of the atmospheric pressure non-thermal plasma system. The tip of the plasma jet that is formed when the argon gas is released and interacts with deionized water and the submerged metal in the beaker is shown in a magnified inset in the figure.

A strip of nickel metal, 7 cm long and 1 cm wide, was Placed in a glass beaker containing 5 ml of deionized water. The plasma nozzle was used 2 cm above the liquid level. Argon gas molecules hit the surface of the liquid within the beaker where surface reactions of the metal gave rise to the metal nanoparticles.

Nanoparticle (NP) preparation took 6 min under argon gas 1.5 l/min and 16-kV applied voltage according to the experiment work. The plasma was created by placing the plasma needle vertically over a beaker with deionized water, in which the metal foil was immersed.

After NiO nanoparticles have been synthesized, thin films were prepared to study their properties. Commercial 3 × 2 cm² glass substrates were used and cleaned with distilled water and alcohol in an ultrasonic bath for 10 min to remove all contamination. Substrates were processed with a nanoparticle solution, using the drop–casting method. This method is frequently used to deposit liquid suspensions of nanoparticles or similar materials onto a surface to make thin films. The specifications of the film required control of the concentration and viscosity of the solution [21].

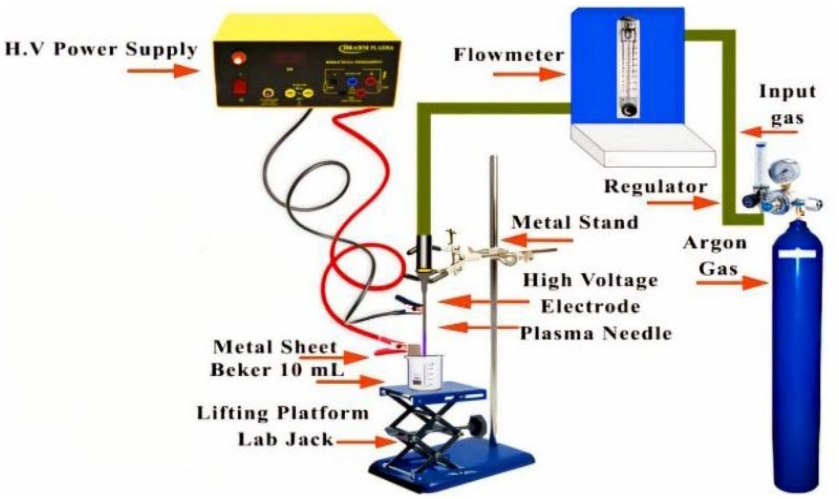

Fig. 1. An illustrative section view of the experimental setup of the atmospheric plasma jet system.

3. Results and discussion

Using X-rays to characterize the crystal structure of materials Naturally occurring crystals It is a phenomenon that allows analyzing the crystal structure of a crystalline material; when X-rays penetrate a crystalline substance, they scatter a certain pattern that reflects the arrangement of atoms. Figure 2 The XRD of NiO nanoparticle film, deposited on glass substrate shown in figure. The peaks in the diffraction results at 2θ = 37.23°, 43.24°,62.74°, and 75.44° that are characteristic of NiO, These planes belong to (111), (200), (220), and (311) reflections respectively, JCPDS file number 00-047-1049[22]. confirms the formation of NiO[15] [22]. It also indicates the cubic phase crystallites of NiO. This indicates the high phase purity of the NiO deposited in this work and no additional peaks were recorded consistent with the AFM, FESE and EDX [23, 24]. The peak XRD details are provided in Table 1. Crystallite size was determined following the Debye-Scherer formula (1) [25, 26].

This also suggests the presence of NiO crystallites with a cubic phase. No extra peaks were detected, demonstrating the excellent phase purity of the NiO synthesized in this study, which is consistent with the AFM, FESE, and EDX results [23, 24]. (see Table 1, the XRD peak details). The average crystallite size was calculated applying the Debye-Scherer formula (1). [25, 26].

$$D = (k\,\lambda)/(\beta\cos\theta) \quad (1)$$

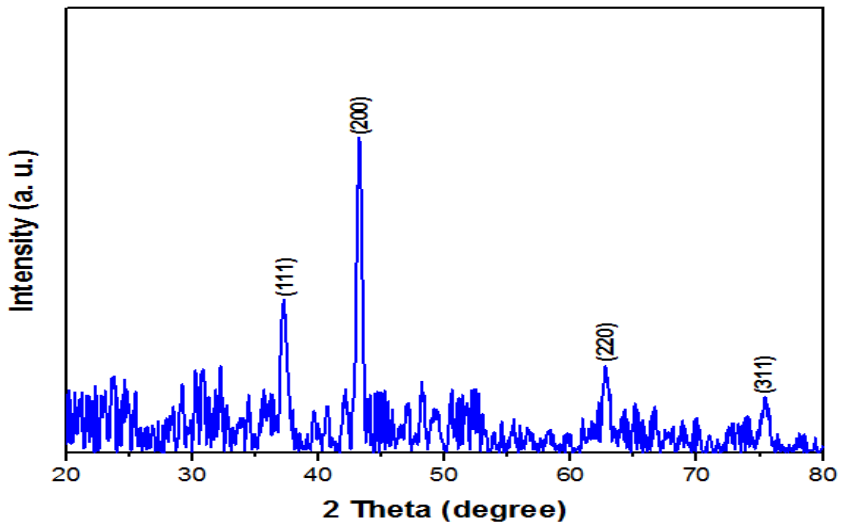

Fig. 2. Schematic diagram for XRD of NiO NPs synthesized by plasma jet.

Table 1. Details of XRD.

Sample	2θ (Deg.)	FWHM (Deg.)	d_{hkl} Exp.(Å)	D (nm)	hkl	Phase
Gas Flow (L/Min) 1.5	37.23	0.6574	2.4132	12.8	(111)	Cub. NiO
	43.24	0.5209	2.0907	16.4	(200)	Cub. NiO
	62.74	0.7097	1.4797	13.1	(220)	Cub. NiO
	75.44	0.7283	1.2591	13.8	(311)	Cub. NiO

Surface topography evolution of NiO nanoparticles (NPs) sample, shown in Figure 3. While the histogram attached is an information regarding the average size of the particles, the 3D image gives information regarding the surface morphology and roughness [114]. Fabricated using the plasma jet method, the NiO thin film showed a flat surface with grains oriented largely perpendicular to the substrate. The surface roughness of the film was established from the height data obtained from the AFM, where the root mean square (RMS) value and grain size was

calculated as the AFM technique is very sensitive to local surface height variations. The measurements gave the parameters of roughness (RMS), (Sa), and mean grain size within the scanning area of 4.72 µm × 4.72 µm as 47.03 nm, 29.59 nm, and 72.65 nm, respectively.

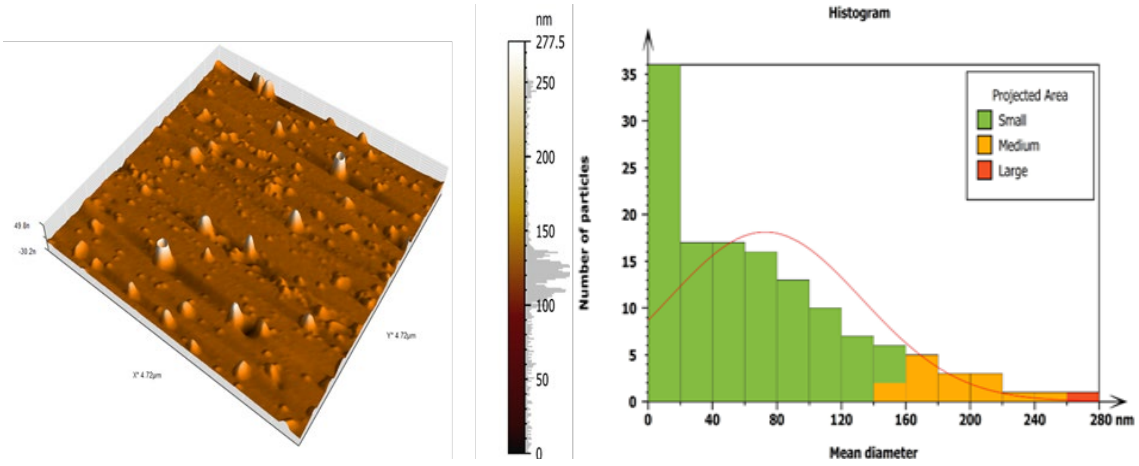

Fig. 3. The 3D image of AFM NiO NPs and histogram distributions prepared by plasma Jet.

The surface microstructure of the NiO nanoparticles is shown in Figure 4. Field Emission Scanning Electron Microscope (FESEM) was utilized to investigate the surface morphology of the NiO nanoparticles prepared via plasma jet method. Different FESEM magnifications of NiO nanoparticles from this work are shown in the figure. According to the image and the zoom view, we realize an intriguing issue, which is the nanostructure of NiO NPs has a few likenesses to that was noticed as little circles, which uncovers the homogeneity of the nanoparticles in size and a decent scattering in the readiness of the NiO NPs test, where the size of the framed nanoparticles expanded between 19.33-38.21nm [27, 28]. Energy-dispersive X-ray spectroscopy (EDX) was utilized to examine the elemental composition of the generated Nickel oxide nanoparticles [29]. The EDX of NiO nanoparticles investigated at a microscope level is shown in Figure 5 along with a Table showing the composition by mass. The respective Mass percent of nickel and oxygen is 80.77 % and 19.23 %, which confirms only presence nickel and oxygen are being analyzed. EDX no more found trace of other elements within the sensitivity range of EDX technique. These results which closely correlate with the XRD data confirm the preparation of pure, highly crystalline NiO nanoparticles. In addition, the ratios measured are consistent with the predicted theoretical values.

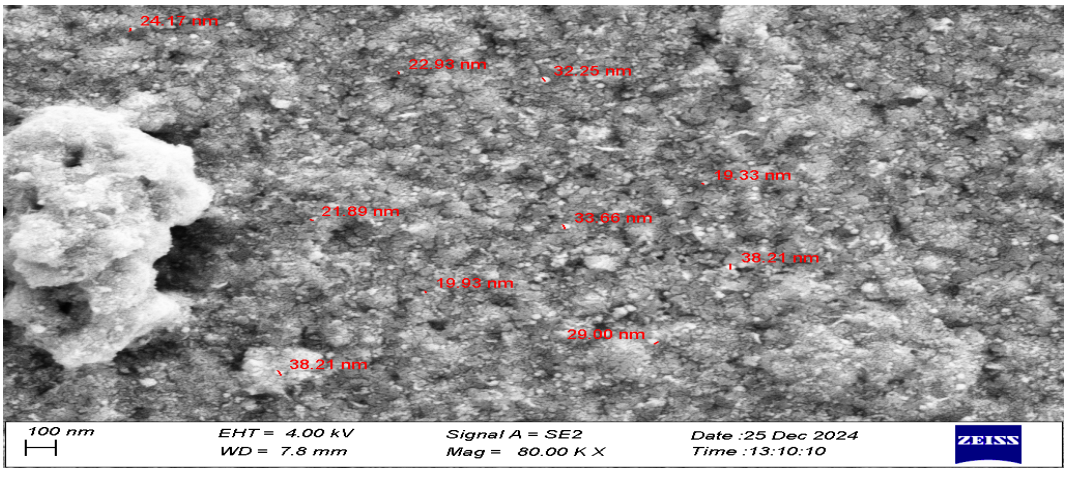

Fig. 4. FE-SEM Images of NiO NPs Synthesized by Plasma Jet.

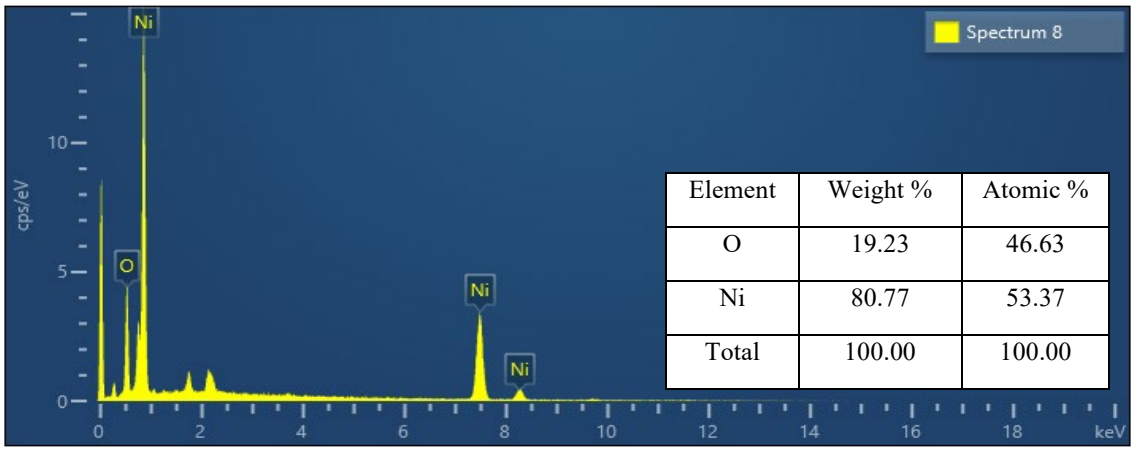

Fig. 5. Shows the (EDX) spectrum of NiO nanoparticles made by a plasma jet.

The UV–vis absorption spectra of NiO nanoparticles are shown in Figure 6. In this case, a unique absorption peak emerges in the deep UV region, with the appearance of a distinct absorption edge inside UV wavelengths. The NiO nanoparticles demonstrate strong UV light absorption, absorbing below 400 nm, which confirms the successful interaction with UV light. The intense absorption edge indicates a high crystallinity and a uniform particle size distribution of the Nanoparticles [28, 30, 31].This acts as a confirmation of the results achieved in the XRD and FESEM tests.

So, the band gap can be found out from the via the equation in the next form, Figure 7 (2).

$$(\alpha h\nu) = A\,(h\nu - Eg)^{n} \qquad (2)$$

where α is the material absorption coefficient, h is a Planck's constant, A is a proportionality constant, ν is the frequency, Eg is the band gap energy, and n is a number that depend on the nature of the electronic transition in the sample, saying direct or indirect in n [32, 33]. 4.05eV is the optical band gap of the material, NiO. The band gap values calculated for NiO nanoparticles are in good agreement with those reported in [34], and the data from the XRD and FESEM analyses.

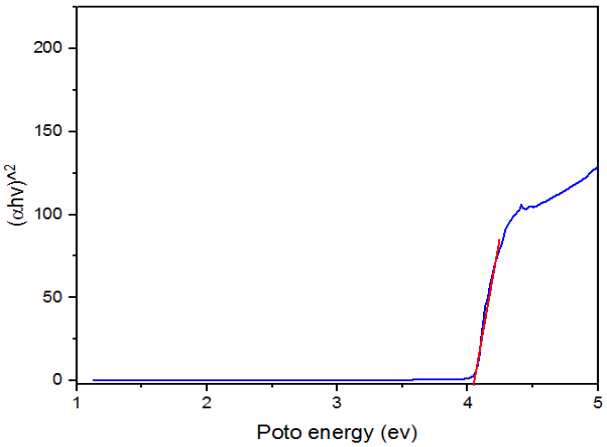

Fig. 6. Optical Absorption Spectrum of Plasma Jet Prepd NiO NPs.

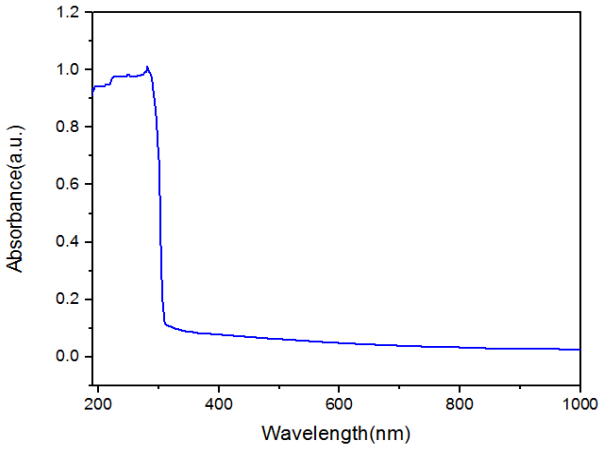

Fig. 7. Optical Bandgap Energy of Plasma Jet Prepd NiO NPs.

4. Conclusion

An inexpensive and environmentally friendly plasma jet process was developed for the synthesis of nickel oxide (NiO) nanoparticles, demonstrating strong potential for scalable applications. The X-ray diffraction (XRD) patterns of the synthesized NiO films revealed characteristic peaks corresponding to the cubic face-centered crystal structure of NiO, confirming successful phase formation and crystallinity.

Atomic force microscopy (AFM) images demonstrated that the film surface is relatively flat, while the grains are stacked in a three-dimensional configuration with perpendicular orientation, suggesting ordered surface morphology and uniform deposition. Complementary to this, field emission scanning electron microscopy (FESEM) images showed that the NiO nanostructures are primarily spherical in shape and exhibit a noticeable degree of aggregation.

The high purity of the metal oxide nanoparticles was validated using energy-dispersive X-ray spectroscopy (EDX), which confirmed the elemental composition of Ni and O without significant impurities. Optical characterization of the NiO nanoparticles revealed an optical band gap (Eg) of 4.05 eV, indicating strong semiconducting properties and suitability for optoelectronic or photocatalytic applications.

References

[1] Thabit, W.S., Al-Rawi, B.K., International Journal of Nanoscience, 2023, 22(2), 2350005; https://doi.org/10.1142/S0219581X23500059

[2] Khathim, S.E., Al-Rawi, B.K., Khalaf, M.K., International Journal of Nanoscience, , 2024, 23(3), 2350073; https://doi.org/10.1142/S0219581X23500734

[3] A. S. Rini, Y. Rati, A. Umar, Nur Adliha Abdullah, International Journal of Nanoelectronics & Materials 13 (2020).

[4] Mustafa, Safa Kamal, Raied K. Jamal, and Kadhim Abdulwahid Aadim, Iraqi Journal of Science (2019): 2168-2176; https://doi.org/10.24996/ijs.2019.60.10.10

[5] Mohammed, S.A.J., Al-Rawi, B.K., Al-Haddad, R.M.S., International Journal of Nanoscience, 2023, 22(2), 2350009; https://doi.org/10.1142/S0219581X23500096

[6] Aadim, K. A., A. Z. Mohammad, M. A. Abduljabbar, IOP Conference Series: Materials Science and Engineering. Vol. 454. No. 1. IOP Publishing, 2018; https://doi.org/10.1088/1757-899X/454/1/012028

[7] Kafel, A., Turki Al-Rashid, S.N., Chalcogenide Letters , 2023, 20(6), pp. 423-429, https://doi.org/10.15251/CL.2023.206.423

[8] Bonomo, Matteo, Journal of Nanoparticle Research 20.8 (2018): 222; https://doi.org/10.1007/s11051-018-4327-y

[9] Sayyadi, Khalilollah, Mahsa Gharani, Abbas Rahdar, Advances in Nanochemistry 1.1 (2019): 34-40.

[10] S. N. T. Al Rashid, Nanoscience and Technology 15, Issue 3, Pages 21 - 27. (2024); https://doi.org/10.1615/NanoSciTechnolIntJ.2023048643

[11] Mallick, P., N. C. Mishra, American Journal of Materials Science 2.3 (2012): 66-71; https://doi.org/10.5923/j.materials.20120203.06

[12] Mahmoud, Safwat A., Alshomer Shereen, A. Tarawnh Mou'ad, Journal of modern Physics (2011); https://doi.org/10.4236/jmp.2011.210147

[13] Mohammed, S.A.J., Al-Haddad, R.M.S., Al-Rawi, B.K., Nanoscience and Technology, , 2024, 15(2), pp. 95-105; https://doi.org/10.1615/NanoSciTechnolIntJ.2023048382

[14] H. A. Abed, S. N. T. Al Rashid, S. N. Mazhir, InternationalJournal of Nanoscience, vol. 22, no. 06, p. 2330005, 2023; https://doi.org/10.1142/S0219581X23300055

[15] Mohammed, Raghad S., Kadhim A. Aadim, Khalid A. Ahmed, Karbala International Journal of Modern Science 8.2 (2022): 88-97; https://doi.org/10.33640/2405-609X.3225

[16] S. N. Mazhir, A. H. Ali, N. Kh. Abdalameer, S. A. Qasim, Inter. J. Nanosc., 21, 3, 2250021. (2022); https://doi.org/10.1142/S0219581X22500211

[17] Hussain, A.M., Al-Rawi, B.K., International Journal of Nanoscience, 2024, 23(3), 2350075; https://doi.org/10.1142/S0219581X23500758

[18] Al-Rawi, B.K., Mazhir, S.N., International Journal of Nanoscience, 2023, 22(5), 2350044; https://doi.org/10.1142/S0219581X23500448

[19] A. Mustafa, S. Turki Al-Rashid, Chalcogenide Letter, Volume 21, Issue 5, Pages 407 - 411May 2024; https://doi.org/10.15251/CL.2024.215.407

[20] Mohammed, S.A.J., Al-Haddad, R.M.S., Al-Rawi, B.K., J Opt (2024); https://doi.org/10.1007/s12596-024-01676-6

[21] Ghdhaib, B. M., S. N. Rashid, Iraqi Journal of Applied Physics, vol. 20, no. 3, 2024, pp. 477-484.

[22] Al-Rawi, B.K., Ramizy, A., Journal of Inorganic and Organometallic Polymers and Materials, 2019, 29(3), pp. 645-650; https://doi.org/10.1007/s10904-018-1037-y

[23] Mohammed, Ghuson H., Iraqi Journal of Science (2022): 2502-2513; https://doi.org/10.24996/ijs.2022.63.6.17

[24] Hubeatir, Kadhim Abid, Eng. Technol. J 34 (2016): 178-185; https://doi.org/10.30684/etj.34.1A.15

[25] Nayef, Uday Muhsin, Kadhim A. Hubeatir, Zahraa J. Abdulkareem, Optik 127.5 (2016): 2806-2810; https://doi.org/10.1016/j.ijleo.2015.12.002

[26] Al-Rawi, B.K., Aljanabi, S.M.H., International Journal of Nanoscience, 2021, 20(1), 2150011; https://doi.org/10.1142/S0219581X21500113

[27] Racik, K. M., J. Madhavan, M. V. A. Raj, National Laser Symposium (NLS-27), RRCAT. 2018.

[28] Hameed, Mohammed M., Abdul-Majeed E. Al-Samarai, Kadhim A. Aadim. Iraqi Journal of Science (2020): 2582-2589; https://doi.org/10.24996/ijs.2020.61.10.14

[29] Md T Uddin, Y Nicolas, C Olivier, W Jaegermann, N Rockstroh, H Junge, T Toupance, Physical Chemistry Chemical Physics 19.29 (2017): 19279-19288; https://doi.org/10.1039/C7CP01300K

[30] Noor, Saima, et al., Journal of Cleaner Production 277 (2020): 123280; https://doi.org/10.1016/j.jclepro.2020.123280

[31] Hameed, Mohammed M., Abdul-Majeed E. Al-Samarai, Kadhim A. Aadim, Iraqi Journal of Science (2020): 2582-2589; https://doi.org/10.24996/ijs.2020.61.10.14

[32] Haq, Sirajul, et al., Journal of Chemistry 2021.1 (2021): 3475036; https://doi.org/10.1155/2021/3475036

[33] Ghdhaib, B. M., S. N. Rashid, Iraqi Journal of Applied Physics, vol. 20, no. 3, 2024, pp. 477-484.

[34] Mahdi, Rana O., et al., AIP Conference Proceedings. Vol. 2213. No. 1. AIP Publishing, 2020; https://doi.org/10.1063/5.0000116